Proceedings World Geothermal Congress 2026
Calgary, Canada, June 8 – 11, 2026

Early-Stage Geothermal Exploration and Characterization Near Kootenay Lake, British Columbia

*Gord MacMahon[1], Daniel Gatto[1], Sonni Greene[1], Leslie Harker[2], Stefan Humphries[2], Lucinda Leonard[3], Theron Finley[3,4,] Daniel Alonso Torres[5], Robert MacQuarrie[6]

1. Kootenay Lake Geothermal Project, PO Box 182, Crawford Bay, BC V0B 1E0, 2. SRK Consulting (Canada) Inc., 320 Granville St #2600, Vancouver, BC V6C 1S9 3. University of Victoria, 3800 Finnerty Road, Victoria, BC V8P 5C2 4. Yukon Geological Survey, 91807 Alaska Hwy, Whitehorse, YT Y1A 0R3, 5. Advection Geo, Suite 1800, 330 5th Avenue SW, Calgary, AB T2P OL4, 6. Selkirk College, 2001 Silver King Road, Nelson, BC, V1L 1C8

*gordmacmahon@gmail.com

Keywords: Geothermal Energy, Exploration, Kootenay Lake, Geophysical Survey, British Columbia, Geothermal Systems, Subsurface, Reservoir Characterization, Thermal Springs, Geochemistry, Geospatial Analysis, Thermal Infrared Survey, UAV Magnetometer Survey, Electrical Resistivity Tomography Survey, Temperature Probes

ABSTRACT

The Kootenay Lake region, located within a high heat flow segment of the North American Cordillera, is located in a post-collisional backarc setting featuring over 20 deep-seated and transtensional faults, many of which host thermal springs associated with Eocene or younger brittle deformation. Geothermal gradients in the area range from 35 to 55°C/km, confirmed by temperature logging in selected wells. The Kootenay Lake Geothermal Project has completed four integrated phases of field exploration that include geological mapping, geospatial analysis, geophysics, and geochemistry focused in the Crawford Creek area and the shores of Kootenay Lake. A drone-based Thermal Infrared (TIR) survey delineated the boundaries of a specific geothermal system, which was further investigated using drone-based magnetometer and ground-based Electrical Resistivity Tomography (ERT) surveys. The geophysical data collected from these surveys provides critical insights into the structural controls and fracture systems facilitating fluid flow within the geothermal reservoir. Geochemical analyses, coupled with geological observations and geophysical interpretations, allows for the generation of preliminary conceptual models for the geothermal systems in the region and exploration prospects. The multidisciplinary approach has refined subsurface interpretations and identified targeted zones of geothermal interest, laying the groundwork for resource estimation and potential future development. The project not only contributes to the understanding of geothermal systems in southeastern British Columbia but also offers a replicable framework for exploration of early-stage geothermal plays.

1 INTRODUCTION

In British Columbia, high temperature geothermal power projects have the potential to produce significant long-term, stable, clean electricity and heat, and there are several geothermal power projects at various stages of development. (i.e. Mount Meager, Mount Cayley, Lakelse, and Mount Edziza).

These high temperature power projects are typically designed to utilize geothermal resources with temperatures greater than 120°C. Lower temperature geothermal systems, in the range of 40 to 100°C can create small scale sustainable economic projects across a spectrum of direct heat commercial applications capable of delivering social and economic benefits straight to the local communities where they are situated. It is this 40 - 100°C range of geothermal temperatures which are the target of this project. Furthermore, it has been shown that geothermal direct heating systems can actually displace more fossil fuel burning than geothermal electricity generation, particularly in cold climates (Lavigne et al. 2020).

The Kootenay Lake project area (Figure 1) is host to several thermal spring occurrences, specifically Ainsworth, Dewar Creek, Riondel and Crawford Creek. Ktunaxa First Nations peoples have experienced the hot springs for millennia and currently own and operate the Ainsworth Hot Springs Resort. In the historic Bluebell Mine at Riondel, temperatures of 40°C and flow rates of 150 litres per second were encountered during mining operations (Desrochers, 1992). Surface temperatures measured at the Dewar Creek hot spring located approximately 30 km northeast of Crawford Bay, exceed 82.8°C (Grasby et al., 2000), making it the second hottest known surface expression of geothermal water in Canada. In addition, geochemical analyses of several hot springs in the Kootenay Lake area indicate that at depths of 2-3 km, water temperatures may exceed 120°C (Grasby et al., 2000). The Kootenay Lake area geology and structure combined with numerous thermal spring expressions, indicates that the region could be prospective for geothermal energy use, prompting us to embark on a multidisciplinary geoscience-based effort to identify a potential geothermal target worthy of inaugural development.

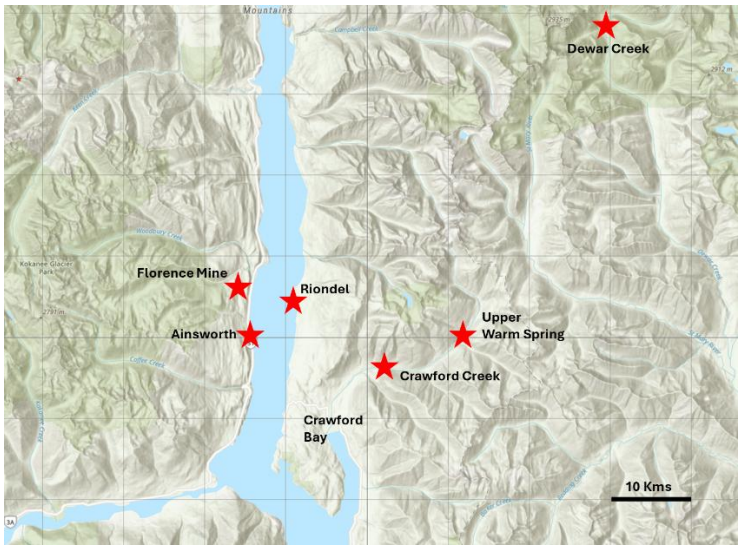


Figure 1. Overview map of the Kootenay Lake Geothermal project study area, showing known thermal occurrences.

2 GEOLOGICAL SETTING

2.1 Regional Setting

The Kootenay Lake region of SE BC exhibits relatively high heat flow (Figure 2). Heat flow mapping illustrates that the modeled heat energy is approximately 25-40% higher than the generalized background within BC and comparable with heat flow values in geothermal producing regions of the SW US (Figure 2). A major physiographic and structural boundary within the Canadian Cordillera occurs at Kootenay Lake, with the Purcell Mountains lying to the east and the Selkirk Mountains to the west of the lake. The Purcell Mountains are underlain by the Purcell Anticlinorium, a large anticlinal structure with some of the oldest rock (Proterozoic) exposures of the Cordillera at its core. The Selkirk Mountains are underlain by the metamorphosed and deformed pericratonic / accreted island arc sequence of the Kootenay Arc (Rioseco & Pattison, 2018).

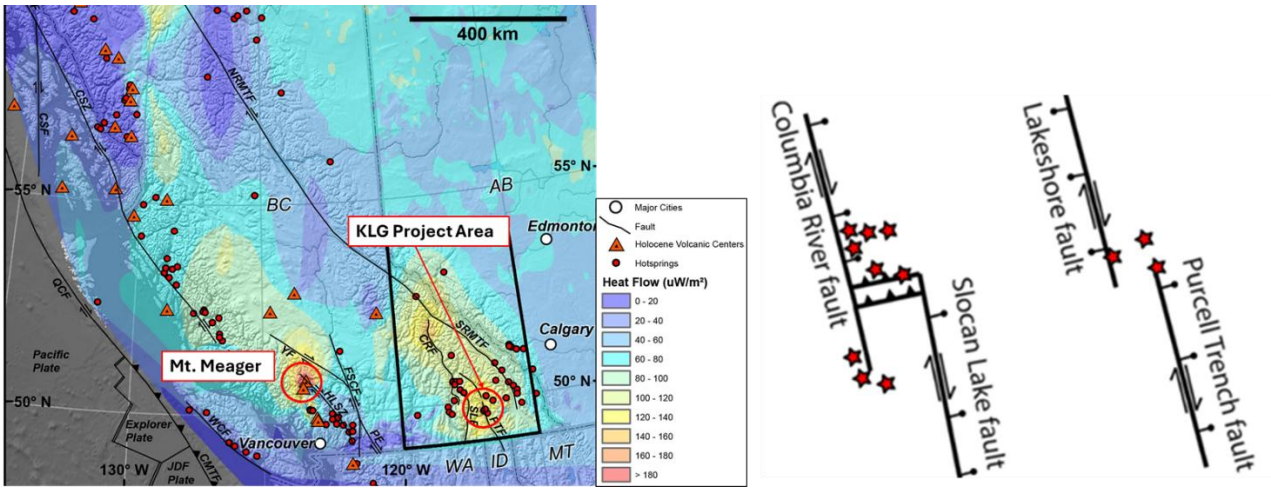


Figure 2. (Left) Map of the Canadian Cordillera showing heat-flow contours modified from Majorowicz and Grasby (2010) and Finley et al. (2022). SRMTF – Southern Rocky Mountain Trench Fault, CRF – Columbia River Fault, SLF - Slocan Lake Fault, PTF – Purcell Trench Fault. (Right) Structural settings of thermal springs in southeastern BC (Finley et al 2022)

The Purcell Trench fault (PTF), which is a major 'down to the east' normal fault, is mapped from Crawford Bay, BC, south along Kootenay Lake, terminating near Coeur D'Alene, Idaho, USA. Initially, the PTF formed as a normal fault under Eocene extension, creating a half-graben geometry. Finley et al (2022) found that bedrock fault kinematics observed along the PTF corridor and other major faults (Southern Rocky Mountain Trench and Columbia River fault zones) in the Kootenays are consistent with the focal mechanisms of modern earthquakes

which have occurred in the region, suggesting that transpressional strain has persisted from the Eocene to recent. The faulting and fracturing produced during this period are thought to maintain fault permeability.

On the west side of Kootenay Lake, the footwall of the PTF hosts a stratigraphic sequence with higher metamorphic grades exhumed from considerable depths, with significant vertical displacement during the Eocene (Moynihan & Pattison, 2013). These rocks are cut by the Midge Creek / Gallagher / Lakeshore fault complex, which extends from the Salmo area in the southwest to north of Kaslo on the west side of Kootenay Lake. Figure 2 (right) shows the position of these regional faults relative to hot springs locations (red stars). Curewitz and Karson (1997) highlighted that fault permeability is higher at strain concentrated areas such as fault intersections. Faulds and Hinz (2015) further characterized transition/transfer zones as favorable sites for geothermal reservoir development.

The geothermal systems found in the Kootenay Lake area can be classified as fault-hosted geothermal systems due to their apparent dependance on fault systems controlling their outlet locations. The Riondel spring is also considered a “blind” geothermal system, as thermal waters do not reach the surface; it has been speculated that other unidentified blind geothermal systems could exist in the Cordillera, where thick vegetation, high annual precipitation, and thick glacial overburden may mask or mute surface thermal expressions (Finley et al., 2022).

2.2 Crawford Creek Geology

East of the village of Crawford Bay, up the Crawford Creek valley, the Crawford Creek thermal spring outlet (32°C) is located near the bottom of the creek valley and within the creek itself. The host reservoir of the thermal spring is inferred to be the Hamill H1, a massive quartzite. To the east, the Hamill H1 overlies the Three Sisters gritstone and quartzite (Hoy, 1980). To the west, it is bounded by the Orebin Creek fault (OCF) and is highly fractured in the vicinity of the fault with persistent occurrence of WNW jointing (strike of ~295° and a dip of 80°). The OCF, a steeply dipping normal fault, separates the Hamill H1 quartzite from the Hamill H2 schist and phyllite (Figure 3).

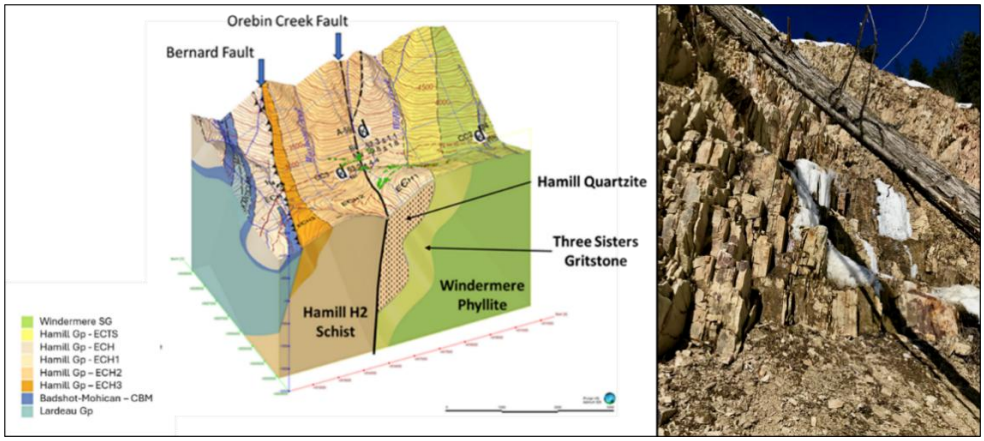


Figure 3. A) Geologic block, looking NNE towards Mount Crawford, modeled after the original bedrock map by Brown, et al. (2011). B) Highly fractured Hamill H1 quartzite in the immediate footwall of the OCF (pictured right).

The 3D geological section shown in Figure 3, shows the Hamill H1 quartzite as it extends north, up to Mount Crawford and it continues north until it contacts the Fry Creek Batholith, approximately 14 kms NNE of Crawford Creek. Steeply dipping bedding with frequent jointing within a brittle quartzite suggests the potential for enhanced permeability with improved conveyance of geothermal fluids from depth in the immediate area, making it a good candidate to study in further detail.

3 EXPLORATION TECHNOLOGIES

3.1 Structural Analysis

Preliminary geological investigations in the early phases of the Kootenay Lake Geothermal Project focused on the Crawford Creek area and included the collection of over 1,000 structural measurements (joints, bedding and faults). Detailed examination of the joint data suggests three distinct joint sets, each with unique orientations and dips. A steeply dipping joint set (70-88°), with an overall WNW (277-313°) strike and increasing joint density

along the projected OCF is the most prevalent. Notably, Moynihan & Pattison (2011) found that the WNW jointing at the Bluebell mine was likely a principal control on both ore placement and the introduction of hydrothermal fluids from depth. Comparing the brittle fractures measured near the Bluebell mine, (Moynihan & Pattison 2011), to the steep Joint Set One fractures measured at Crawford Creek in Figure 4 shows a good correlation, suggesting similar structural influences.

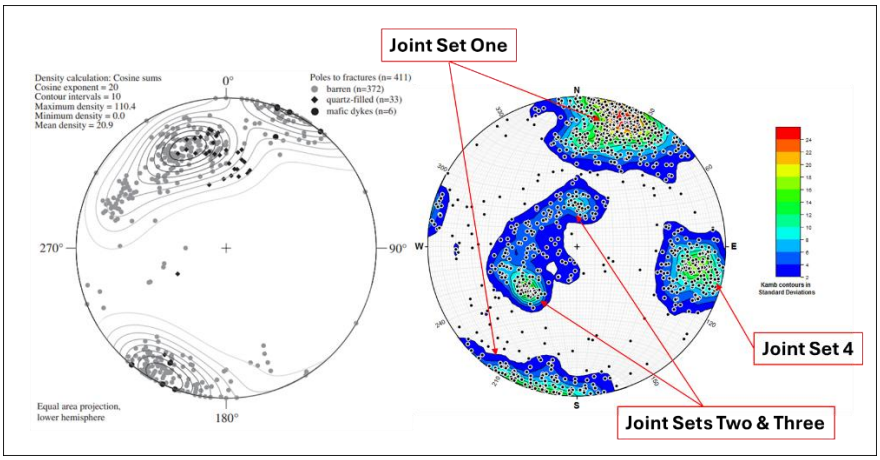


Figure 4. Equal area lower hemisphere stereonet showing contoured poles to brittle fractures in the Hamill Group (hanging wall), directly to the west of the Comfort and Bluebell ore zones at Riondel (Moynihan & Pattison, 2011), (left); compared to the four joint sets measured in the Hamill Fm. at Crawford Creek (right).

Another prominent set of steeply-dipping joints (Joint Set 4) have a NNE orientation (10-20°). The remaining two joint sets are more gently dipping and observed mostly north of Crawford Creek where the strike of the OCF shifts from NS to NNE-SSW. Joint Set Two has a strike of 282-303° and a dip of 45-55° and Joint Set Three has a strike of 110-211° and dip of 45°.

3.2 Geochemical Sampling and Analysis

A geochemical sampling campaign was undertaken to better understand the source and pathways of the geothermal waters at Crawford Creek. Figure 5 shows the locations of the sample sites and the approximate position of the Orebin Creek Fault. Sample sites with a black triangle indicate there was a measured thermal influence and are sourced within the area underlain by the Hamill H1 quartzite. As these sites were regularly tested through the summer field season it was apparent that the thermally influenced waters with the H1 quartzite had low TDS and Conductivity along with slightly lower pH (6.2-7.0). Stepping outside the thermally influenced area the TDS, pH and conductivity were all observed to increase, while temperature decreased. This speaks to the rather local nature of the thermal waters at Crawford Creek (thermally influenced waters were >16°C compared to surface flow of 10-12°C). Samples collected within the H2 schist were west of the OCF and outside the thermally influenced area.

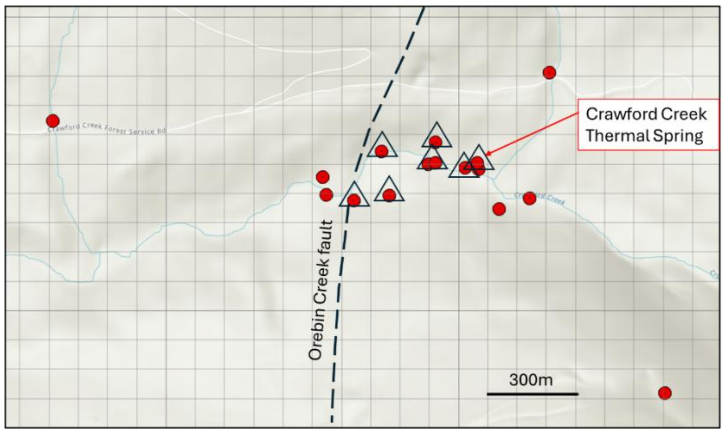


Figure 5. Geochemical sampling sites at Crawford Creek (2022-2025), shown by red circles. Sites with measured thermal influence shown by black triangles.

The Crawford Creek thermal seeps and springs all had proportionally higher dissolved fractions of sulfate, sodium and potassium, and lower calcium compared to surface water. Given the chemical consistency and absence of indicators of mixing, the geochemical data from these springs suggests that the water may be primarily interacting with quartzites and derived from meteoric sources, as evidenced by comparatively low mineral concentrations and meteoric water isotopic composition (SRK Consulting (Canada) Inc., 2023). In contrast, groundwater emerging from carbonate rocks, such Ainsworth Hot Springs, and the Bluebell Mine at Riondel show higher salinities dominated by bicarbonate alkalinity, sulfate, calcium, sulfate, and sodium.

Sampling for helium and neon isotopes was conducted in 2024 with follow-up at Crawford Creek in 2025, since He, Ne isotope ratios can provide an indication of the source of the geothermal fluid (Torgersen & Jenkins, 1982; Pyle, 1993). Helium and neon samples were collected at Dewar Creek, the Upper Warm Spring (UWS, a newly discovered thermal spring), Crawford Creek and Ainsworth. The samples from the UWS (R/Ra of 0.75) and Dewar Creek (R/Ra of 0.48) have excess He, dominated by 4He (crustal), but with minor additions of 3He (magmatic), while Ainsworth Hot Spring samples (R/Ra of 1.59) indicated a great mantle influence (Alonso Torres, 2025). The sample from Crawford Creek displayed atmospheric values and was suspected to be contaminated. It was resampled in 2025 with results indicating mainly crustal influence (R/Ra of 0.3-0.4).

3.3 Drone-based Thermal Infrared (TIR) survey

To improve mapping of the surface expression of the Crawford Creek thermal spring, a drone-based Thermal Infrared (TIR) survey was conducted. The aerial TIR imagery was collected using Zenmuse H20T (thermal) sensors mounted on a DJI Matrice 300 RTK drone. The survey was conducted after dark, late in the month of October (before snow cover), when there would be a greatest temperature differential between ambient air and surface.

The preliminary thermal mosaic shows a surface geothermal expression which extends beyond the primary spring, up and down the valley for a total of 300 m and over 55 m upslope from the valley bottom (Figure 6).

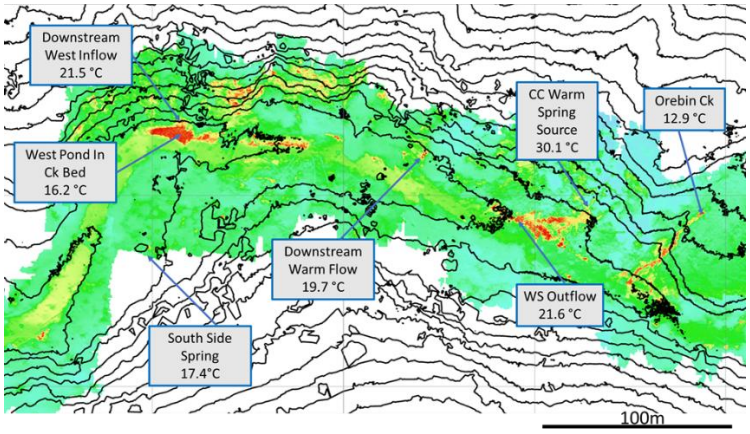


Figure 6. Surface verification of thermal seeps and springs detected using TIR thermal imaging. Results recorded in 2023 are overlain on thermal mosaic (measured non-thermal surface waters were typically 10-11°C)

During the following summer (2023), field explorations verified the anomalous thermal readings; however some of the seeps low in the creek valley and in the creek bottom were not detectable until later in the summer when the creek water level was considerably lower. Downstream of the main warm spring at Crawford Creek, the westernmost thermal anomaly was completely submerged under early summer creek flow and no thermal water was found. By mid-July however, a warm inflow was detected under a fallen tree with a measured temperature of 21.5°C.

It is apparent that thick tree cover made detection of surface thermal features difficult. Most of the anomalous signatures observed directly were situated in more open areas such as the creek edges and the creek bottom itself. The anomalous TIR features located on very steep terrain in the western half of the survey could not be confirmed due to the sheer cliffs in that area. There was a very small (2°C) change in water temperature in the lower 50m of Orebin Creek, but the actual source of this temperature difference could not be determined.

3.4 Drone-based Magnetometer survey

A drone-based magnetometer survey was conducted to better image the local geological structures in the vicinity of the Crawford Creek thermal spring. Geotronics Consulting Inc, based in Kaleden BC, were on site in October 2023 to conduct a survey covering an area of about 1.5 km^2. The magnetometer used for the survey was a GEM Systems potassium type, model GSMP-35U. Mounted with the magnetometer was a laser altimeter for measuring terrain clearance and a GPS unit for measuring the UTM location to an accuracy of 0.7m.

The OCF is indicated with a dashed yellow line on Figure 7. Of note is how the fault trends N-S until it approaches Crawford Creek where it bends clockwise to a NNE-SSW (~21-23°) orientation. Note that 21-23° is approximately aligned with the regional NNE-SSW orientation of SHmax (Finley et al 2022). Feature A on the First Vertical Derivative map (Figure 7), lies just east of the OCF within the highly fractured Hamill H1 quartzite, representing a NNE-SSW zone of low magnetic susceptibility in the immediate footwall of the OCF. Feature B, a WNW-ESE trending zone of low magnetic susceptibility that is coincident with the Crawford Creek valley as well as the strong lineament on the Horizontal Derivative map (Figure 7).

In addition, there are prominent NNE-SSW trending features with strong vertical and horizontal contrasts. These features seem to follow the OCF and are oriented parallel to the regional NNE-SSW S_{Hmax} (~21-23°) and could represent zones of low magnetic susceptibility possibly due to greater degrees of fracturing.

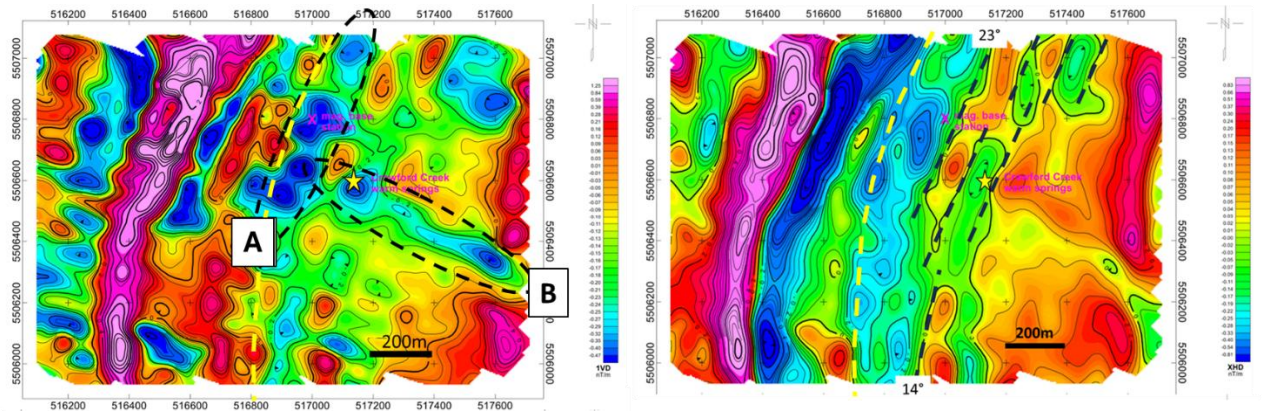


Figure 7. First Vertical Derivative map (left), First Horizontal (EW) Derivative map (right) Geotronics Consulting Inc. (2023). Interpreted structural lineaments are shown as black dashed lines, approximate location of OCF shown as dashed yellow line.

The maps of first horizontal derivative – which is a measure of the horizontal rate of change of the Total Magnetic Field, highlight the edges of features such as contacts or faults. A major WNW-ESE (296-299°) trending lineament follows the trend of the Crawford Creek valley and is very evident on the first horizontal (Y) derivative (north-south) maps. This WNW-ESE orientation is the same orientation as Joint Set One (Figure 4) - and shares a similar orientation to an important joint set at the nearby Bluebell Mine.

3.5 Ground-based Electrical Resistivity Tomography (ERT) survey

An AGI SuperSting electrical resistivity tomography (ERT) system was used to image the electrical properties of the subsurface in the vicinity of the Crawford Creek thermal spring. The SuperSting system is equipped with 112 electrodes and over 1,000 m of cable, allowing for a maximum potential depth penetration of ~250 m. A dipole-dipole array configuration was selected to maximize resolution of lateral variations in the subsurface.

The electrical resistivity of rocks is quite variable (Palacky, 1988) and observed values ranged several orders of magnitude with considerable variability even within individual rock types. The rocks encountered in the Crawford Creek vicinity are composed of silicates predominantly, which typically have relatively high resistivity (low conductivity). Pore space and fluid saturation, however, can lower the resistivity of bedrock significantly.

In August 2023, three ERT survey lines were conducted as follows: 1) a ~1,000 m long approximately W-E survey along the Crawford Creek Forest Service Road (FSR) with 10 m electrode spacing, 2) a 250 m long ~W-E survey on the north bank of Crawford Creek with 5 m electrode spacing, and 3) a 250 m long ~S-N survey perpendicular to profiles 1 and 2, with 5 m electrode spacing. These survey lines were designed to cover all surface warm spring outlets and major geological features of interest (i.e., the OCF). Due to space limitations, only profiles 1 and 2 are shown and discussed here.

In the Crawford Creek Forest Service Road (FSR) (Figure 8-top) profile, the near surface low resistivity features on the FSR section west of the OCF are interpreted to correlate to the Hamill H2 (micaceous schist and phyllite) which hosts some localized occurrences of sulfides or clay rich intervals in surface outcrops. There is a significant low resistivity feature, located near the middle of the FSR section (C4 in Figure 8), vertically beneath and just east of an outcrop exposure of the OCF and within the mapped (and highly fractured) Hamill H1 quartzite. This feature (C4) occurs mostly between elevations of 660m and 580m, approximately 140 m below the road surface. Another low resistivity feature (C5 on Figure 8) is evident near the eastern end of the profile but considerably shallower, at 805-790 m. This is a lower confidence feature being right at the edge of the profile.

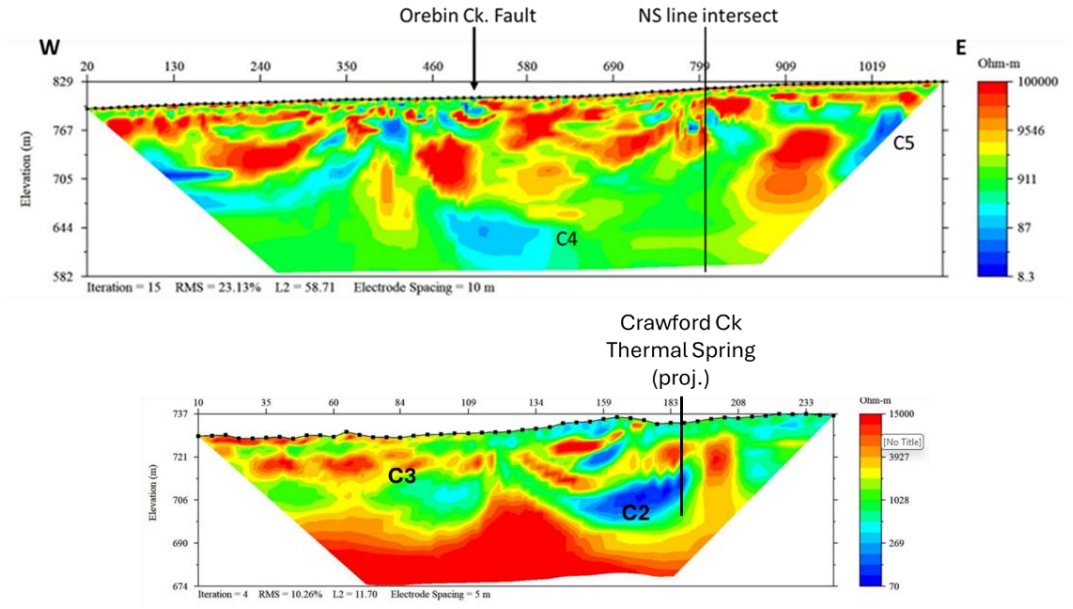


Figure 8. ERT Inverted Resistivity Sections (elevation corrected) – Crawford Creek FSR (top): 10m electrode spacing 10m, length ~ 1.2 km, Crawford Creek Bank (bottom): 5m electrode spacing, length ~250m B. Worsnop, UVic November 2023 (elevation corrected). Note different Hz scales for the two profiles.

The Crawford Creek bank profile (Figure 8-bottom) extended from the small alluvial fan at the confluence of Orebin Creek with Crawford Creek westward to the Hamill H1 quartzite cliff band. This section passed immediately south of the Crawford Creek thermal spring outlet (C2), crossing over an interval of slumped glacial till and past the western warm outflow, which emerges under the cliff band just north of the creek (C3). Note that conductor C3 is located near the warm outflow (20°C) and situated very close to a temperature probe (Site #8) which also showed the highest determined heat flow in the immediate area (Figure 9).

3.6 Temperature Probes

To better understand the distribution of thermal anomalies detected by the drone-based TIR survey, an array of temperature probes was used to measure near surface heat flow at the Crawford Creek site. In an earlier Mt. Meager study, Chen et al (2022) recognized that the most accurate ground surface temperatures are derived in the winter months as the snow cover removes solar impacts and allows for an estimation of actual geothermal heat flow using a multiple sensor configuration in the monitoring network. These heat flow estimates could then be used to characterize any observed temperature anomalies and their potential relationship to subsurface geothermal heat sources.

In 2023, temperature probes were provided by the Geological Survey of Canada (GSC), programmed and ready to record ground surface temperature every 30 min. These miniature temperature data loggers (HOBO Water Temp Pro-v2) are durable and waterproof with the ability to record temperatures with an accuracy of ±0.2°C. They were deployed in July 2023 and recovered in July 2024. Twenty-two sites saw two probes buried at each site, one at a depth of 40-50 cm and another probe at a depth of just 3-5 cm (Figure 9).

When the data loggers were recovered, a measurement of soil moisture was documented and a soil sample, of approximately 10 cm in diameter, was collected in a metal tube, sampling a column of soil ~15-20 cm in length for 12 of the 22 sites. The soil samples were analyzed by the Institut National de la Recherche Scientifique (INRS) lab in Quebec using a KD2 pro needle probe for soil thermal conductivity and diffusivity analysis. Sites where the

soil was not sampled and analyzed were assigned assumed soil properties based on soil type. With the INRS data, Zhuoheng Chen and his colleague Wanju Yuan, at the GSC utilized the year-long temperature data to estimate the heat flow at the sites in question. The mean heat flow calculated ranged from 1.0 to 17.3 W/m2 with the highest value determined at site #8 near the warm spring located approximately 145 m downstream of the Crawford Creek warm spring.

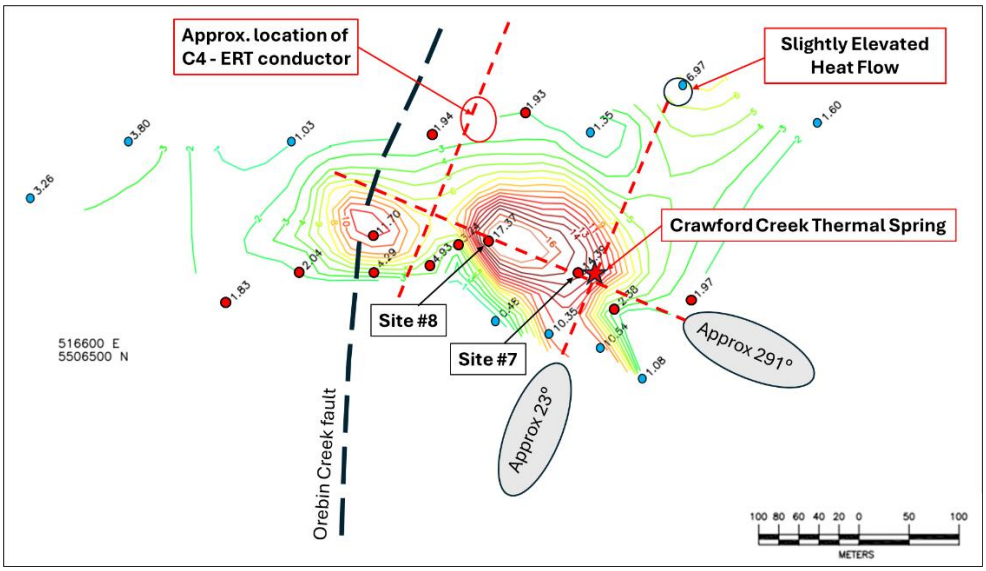


Figure 9. Contour of heat flow estimate (W/m^2), calculated from temperature probe and thermal conductivity data (GSC, 2024). OCF shown with black dashed line, inferred fracture trends shown with dashed red lines. Red dots indicate soil sampled/analyzed, blue dots indicate soil not analyzed, assumed values used in heat flow calculation. Note that sample site #8 was at the lowest elevation in the valley.

The second highest value (14.4 W/m2) was determined for site #7 which was located beside the Crawford Creek thermal spring. Figure 9 shows a contour of the calculated heat flow results, highlighting the potential relationship between fracture trends and the location of some of the conductive features observed on ERT profiles in the vicinity.

4 RESULTS & SUGGESTED MODEL

A preliminary conceptual model for the Crawford Creek geothermal system has been developed considering regional geological mapping, local structural data, aqueous geochemical sampling, airborne and ground-based geophysical surveys, and thermal anomaly measurements. This conceptual model will form the basis of further exploration. The regional geological map (Brown et al., 2011) indicated that the Crawford Creek geothermal system is in the immediate footwall of the OCF, a steeply-west-dipping normal fault. The main outlet of the thermal spring, as well as subsidiary distal outlets revealed by TIR imagery and ground temperature probes, all appear to emanate from within the mapped boundary of Hamill H1 quartzite. Detailed structural analysis completed as part of this project revealed that the Hamill H1 is highly fractured and jointed, with a dominant set of WNW-ESE joints sharing a similar orientation to geothermal-fluid-bearing fractures at the nearby Bluebell Mine. Further examination of results revealed pronounced NS jointing parallel to bedding and parallel to the OCF.

The aeromagnetic surveys confirm the overall NNE-SSW structural fabric of the Crawford Creek valley and indicate a prominent NS lineament that corresponds to the regional orientation of S_{Hmax} and the preferred orientation for potential fracture dilation. Ground-based ERT surveys successfully image a conductive feature interpreted as the hydrothermal plume directly beneath the main spring outlet. Moreover, a low resistivity feature imaged ~140m below ground ~175 m north of the spring outlet, could represent a feeder of the hydrothermal system, wherein warm water is flowing south along the structural grain, and reaching the surface near the intersection of the OCF and the WNW-ESE fracture that follows (and likely controls) the Crawford Creek valley.

Geological modelling has provided a plausible 3D geometry of major geological units in the study area, indicating that the Hamill quartzite forms a NNE-SSW striking wedge that terminates ~1500m below ground against the OCF (Figure 10). The geochemical analysis results from the Crawford Creek warm springs suggested that thermal waters, although likely diluted by surface water flow, have probably not originated from great depths,

but instead have evolved through a shallow geothermal or low enthalpy system. Furthermore, the thermal water contained low dissolved solids, suggesting that it has mainly flowed through the non-reactive Hamill H1 quartzites.

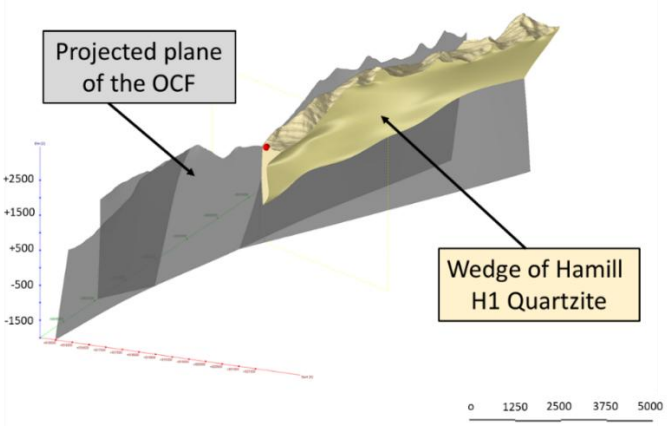


Figure 10. Conceptual 3D model showing the Hamill H1 quartzite wedge extending north from the Crawford Creek warm spring (red dot) up Mount Crawford and beyond. The plane of the OCF is grey.

A shallow or low enthalpy system in this area most likely has meteoric recharge at elevation (i.e. mountain top regions). The mountains above Crawford Creek warm springs represent an elevation gain of just over 1,600 m. At a geothermal gradient of 3.5°C per 100 m, the temperature of meteoric water could increase by 56°C as it percolates through the mountain to the outlet at Crawford Creek, acknowledging that the geothermal gradient may be more gradual beneath mountains. The current conceptual model suggests that the Hamill quartzite at Crawford Creek could extend down another 1,500 m, however even an additional 500 m of circulation at depth would result in a fluid temperature increase an additional 17°C. Assuming an average water temperature of 0°C upon entry, it further suggests that the circulating fluids may reach temperatures of 75°C or greater, within this system. This value closely matches the temperature of 74°C calculated using the quartz geothermometer of Fournier (1977) from stoichiometric conversions of silicon measured at the Crawford Creek warm springs.

5 CONCLUSION

The geophysical data collected from these surveys provides important insights into the structural controls and fracture systems facilitating fluid flow within a near-surface geothermal reservoir. This multidisciplinary approach has refined subsurface interpretations and identified a potential geothermal reservoir within the fractured Hamill H1 quartzite at Crafword Creek, laying the groundwork for resource validation and potential future development. In combination these off-the-shelf technologies can be readily deployed in a cost effective, focused manner once the regional geology and prevailing structural conditions are better understood. This methodology can assist in advancing the development of shallow geothermal reservoirs for direct-use while enhancing a prospective subsurface model for potential deeper and higher temperature geothermal targets. A commercial direct-use geothermal development could attract investment, stimulating economic development and provide clean energy jobs within the local community.

REFERENCES

Alonso Torres, D. (2025). Review of geoscience data for the Kootenay Lake Geothermal Project. Prepared for South Kootenay Lake Community Services Society, Crawford Bay, BC.

Brown, D.A., Wagner, C.L., and Chow, W., (2011). Geology, Crawford Bay, British Columbia; Geological Survey of Canada, Open File 6307

Chen, Z., Grasby, S., Yuan, W., and Liu, X. (2022) Ground surface temperature monitoring data analysis and applications to geothermal exploration in volcanic areas, Mount Meager, western Canada, Geothermics 108 (2023) 102610, https://doi.org/10.1016/j.geothermics.2022.102610

Chen, Z., Grasby, S. E., Yuan, W., Lu, D., & Deblonde, C. (2025). Identification of geothermal anomalies from Landsat derived land surface temperature, Mount Meager volcanic complex, British Columbia, Canada. Remote Sensing of Environment, 320, 114649. https://doi.org/10.1016/j.rse.2025.114649

Curewitz, D. & Karson, J.A. (1997). Structural settings of hydrothermal outflow: Fracture permeability maintained by fault propagation and interaction. Journal of Volcanology and Geothermal Research, 79(3–4), 149-168. https://doi.org/10.1016/S0377-0273(97)00027-9

Desrochers, D.T., (1992) Geothermal Feasibility Study for the Use of Hot Water Near Riondel, British Columbia, Geological Survey of Canada Open File 2502

Faulds, J. E., & Hinz, N. H. (2015). Favorable tectonic and structural settings of geothermal systems in the Great Basin region, western USA: Proxies for discovering blind geothermal systems. In Proceedings, World Geothermal Congress 2015, Melbourne, Australia. Nevada Bureau of Mines and Geology, University of Nevada, Reno. (DOE-UNR-06731-02).

Finley, T. D., Johnston, S. T., Unsworth, M. J., Banks, J., & Pana, D.-I. (2022). Modern dextral strain controls active hydrothermal systems in the southeastern Canadian Cordillera. GSA Bulletin.

Fournier, R. O. (1977). Chemical geothermometers and mixing models for geothermal systems. Geothermics, 5(1–4), 41–50.

Fyles, J. T. (1967). Geology of the Ainsworth-Kaslo Area, British Columbia. Bulletin 53. British Columbia Department of Mines and Petroleum Resources.

Georgsson, L. S., (2009) Geophysical Methods Used in Geothermal Exploration, United Nations University Geothermal Training Programme, Reykjavik, Iceland

Geotronics Consulting Inc., (2023). Geophysical Report on a UAV Magnetic Survey Over the Kootenay Lake Geothermal Project Area, Crawford Bay British Columbia

Grasby, S.E., I. Hutcheon and H.R. Krouse, (2000) The Influence of Water-Rock Interaction on the Chemistry of Thermal Springs in Western Canada. Applied Geochemistry, Vol. 15, p. 439-454.

Grasby, S.E. and I. Hutcheon, (2001) Controls on the Distribution of Thermal Springs in the Southern Canadian Cordillera. Canadian Journal of Earth Sciences, Vol. 38, p. 427-440.

Höy, T. (1980). Geology of the Riondel Area, Central Kootenay Arc, Southeastern British Columbia. Bulletin 73. British Columbia Ministry of Energy, Mines and Petroleum Resources.

Lavigne, C., Guthjónsdóttir, M., & Banks, J. (2020). Heat or power: Proposing geothermal development on the basis of fossil fuel displacement. Proceedings of the World Geothermal Congress 2020, 13.

Moynihan, D.P., and Pattison D.R.M., (2013) Barrovian Metamorphism in the Central Kootenay Arc, British Columbia: Petrology and Isograd Geometry, Canadian Journal of Earth Science 50: 769–794

Moynihan, D.P., and Pattison D.R.M., (2011) The Origin of Mineralized Fractures at the Bluebell Mine Site, Riondel British Columbia, Society of Economic Geologists, Inc., Economic Geology, v. 106, pp. 1043–1058

Palacky, G. J. (1988). Resistivity Characteristics of Geologic Targets. In Electromagnetic Methods in Applied Geophysics (Vol. 1, pp. 53-129). Tulsa, OK: Society of Exploration Geophysicists. https://doi.org/10.1190/1.9781560802631.ch3

Pyle, D. M. (1993). Graphical analysis of rare gas mixing systematics in geothermal systems. Geochemical Journal, 27(2), 125–129.

Rioseco, N.A. and Pattison, D.R.M. (2018): Preliminary investigations of the metamorphic and thermochronological interface between the Purcell Anticlinorium and the Kootenay Arc, southeastern British Columbia (NTS 082F, G); in Geoscience BC Summary of Activities 2017: Minerals and Mining, Geoscience BC, Report 2018-1, p. 47–56.

SRK Consulting (Canada) Inc. (2023). Results and interpretation of the Phase 3 water quality sampling program (Final). Prepared for South Kootenay Lake Community Services Society, Crawford Bay, BC. Project No. CAPR002883. Issued December 8, 2023.

Torgersen, T., & Jenkins, W. J. (1982). Helium isotopes in geothermal systems: Iceland, The Geysers, Raft River and Steamboat Springs. Geochimica et Cosmochimica Acta, 46(4), 739–748.

Webster, E.R. and Pattison, D.R.M., (2013) Metamorphism and Structure of the Southern Kootenay Arc and Purcell Anticlinorium, Southeastern British Columbia (Parts of NTS 082F/02, /03, /06, /07); in Geoscience BC Summary of Activities 2012, Geoscience BC, Report 2013-1, p. 103–118.